Biosorption of uranium(VI) from aqueous solution using phosphate-modified pine wood sawdust

Limin Zhou · Zhiwei Huang · Taian Luo ·
Yuyan Jia · Zhirong Liu · Adesoji A. Adesina

Abstract The phosphate-modified pine wood sawdust (PA-PWS) was used as a biosorbent for U(VI) adsorption from aqueous solution. FTIR analysis indicated that the carboxyl groups and the phosphate groups might be responsible for the adsorption of U(VI) onto PA-PWS. The equilibrium data were correlated with Langmuir and Freundlich models, and the maximum monolayer adsorption capacity obtained from the Langmuir model was 74.1 mg/g at 293 K. The influence of particle size, sorbent dosage, and U(VI) concentration on the adsorption kinetics was evaluated. In most cases, both the sorbent dosage and the metal concentration had great impact on the kinetic parameters (adsorption capacity and rate constant), while the particle size only had limited effect on these parameters.

Keywords Pine wood sawdust · Phosphate · Uranium(VI) · Biosorption

Introduction

Uranium has important applications including nuclear power production, military applications (e.g., nuclear weapons, depleted uranium penetrators, armored vehicles), electron microscope parts as well as glass and pottery glaze. Uranium is extremely dangerous for the environment and human health due to its high toxicity even at very low concentrations and long half lives. Once inhaled or ingested, uranium is mainly toxic for the kidneys and may severely affect their function. Its radioactivity also poses increased risks of lung cancer and bone cancer [1]. The USEPA has classified uranium as a confirmed human carcinogen and suggests that zero tolerance is the only safe acceptable limit [2]. Removal of uranium from the wastewaters is still problematic and represents a great challenge for the researchers [3].

The conventional methods for the separation of radioactive ions from aqueous solution include chemical precipitation [4], ion exchange [5], solvent extraction [6], membrane-related processes [7], biological processes [8] and adsorption [1–3, 9–13]. Among the all above methods adsorption is highly effective and economical [9]. The synthetic resins are expensive and may be difficult to eliminate at the end of their life cycle. Biosorption is presented as an alternative method for removing toxic metals from wastewater [3]. The biomass by-products, such as rice straw, wood sawdust, and wheat straw, represent important resources for biosorption processes. These renewable resources are characterized by the presence of a number of active sorption groups similar to those found on conventional resins and they can be used for metal binding through different reactions including ion exchange, electrostatic attraction, complexation [10–13]. Moreover, the treatment of the waste sorbents is simple and less hazardous in terms of elimination at the end of their life cycle (pyrolysis and incineration for example) [14]. Various natural resource materials such as *Saccharomyces cerevisiae* [3], *Hydrilla verticillata* [10], *Cyanobacterium bloom*

L. Zhou (✉) · Z. Huang · T. Luo · Y. Jia · Z. Liu
State Key Laboratory Breeding Base of Nuclear Resources and Environment, East China Institute of Technology, Nanchang 330013, People's Republic of China
e-mail: minglzhecit@sohu.com

A. A. Adesina
School of Chemical Sciences and Engineering, University of New South Wales, Sydney 2035, Australia
e-mail: a.adesina@unsw.edu.au

[11], *Pseudomonas strain* [12], *Catenella repens* [13], olive cake [15] and citrus waste biomass [16] have been used for uranium uptake applications.

Pine wood sawdust (PWS) is a waste by-product of the timber industry that is either used as a cooking fuel or a packing material, but this biomass was also tested for the sorption of heavy metals [17], and more recently for removal of malachite green [18]. Sawdust can be used as a low-cost adsorbent largely due to its lignocellulosic composition. It is a highly fibrous material made of cellulose, hemicelluloses and lignin plus a non-negligible percentage of ash. The abundant functional groups such as carboxyl, hydroxyl, phenolic, and amide groups present in the sawdust make the adsorption processes possible [17, 18]. The PWS can be used as raw materials but the sorption capacities of them are generally low. Modification of PWS could be carried out to improve structural durability, enhance adsorption capacity or selectivity, and add value to the by-products [18]. Phosphate groups are known to have good affinity for uranium since the UO_2^{2+} could chelate with the phosphate groups of the resins to form complex structure [19]. Thus the modification of phosphate with PWS may improve its adsorption for uranium from aqueous solution.

This work aims to investigate the feasibility of using phosphate-modified PWS for the removal of uranium(VI) ions from aqueous solutions. The effects of different parameters such as initial pH, shaking time, initial metal concentration, particle size and sorbent dosage on the sorption were investigated. The sorption isotherms and kinetics were discussed according to different theoretical models.

Materials and methods

Preparation and characterization of the sorbents

PWS (collected from New South Wales, Australia) was used as biomass feedstock. The wood biomass was dried in a vacuum oven at 70 °C for 24 h. The biochemical compositions (determined by Klason sulfuric acid digestion procedure [20]) of the PWS are: cellulose 49.9 %, hemicellulose 19.7 %, lignin 24.9 % and others 5.5 %. Dried biomass was finally crushed and sieved according the following size fractions (SF): 0–80 μm (*D*1)/80–140 μm (*D*2)/140–250 μm (*D*3)/250–500 μm (*D*4).

The phosphate-modified pine wood sawdust (PA-PWS) was obtained by the following procedures: 10.0 g of PWS were agitated with 100 mL of 0.5 M H_3PO_4 solution for 24 h. After that the treated PWS was separated by filtration and rinsed four times with demineralized water, before being dried in an vacuum oven at 70 °C for 24 h.

The zeta potential measurements were performed using a Zeta Potential Analyzer 2000. FTIR spectra of the sorbents were measured on a Nicolet, Magna-550 spectrometer.

Reagents

The stock solution of U(VI) (500 mg/L) was prepared by dissolving accurately weighed amount of $UO_2(NO_3)_2$·$6H_2O$ in deionized water, after adding some drops of HNO_3 to accelerate the dissolution of the reagents. Arsenazo III (A.R. grade) was purchased from Aldrich.

Determination of U(VI) in solution

The concentration of U(VI) was determined by Arsenazo-III spectrophotometric method using a Shimadzu UV-1601 spectrophotometer. 1 mL U(VI) solution sample, 5 mL chloroacetic acid ($ClCH_2COOH$)–sodium acetate (CH_3COONa) buffer solution (pH 2.5) and 1.0 mL 0.1 % Arsenazo-III aqueous solution were added to a glass flask subsequently, the final solution volume was filled up to 25 mL by adding deionized water. After 10 min, the absorbance of the mixture liquid was measured at 650 nm.

Adsorption of U(VI) ions

Effect of pH

Uptake experiments were performed at controlled pH (2.0–6.5) and 298 K by shaking 50 mg of biomass (SF: 140–250 μm) with 100 mL of 50 mg/L U(VI) solution at different pH values. The initial pH values of the working solutions were adjusted by adding 0.5 mol/L HNO_3 or 0.5 mol/L NaOH solutions. After 24 h of agitation time (150 rpm) each solution was filtered using a 0.45 μm syringe mounted filter. The residual U(VI) concentration after adsorption was determined.

Adsorption isotherms

Sorption isotherms were performed by contact of 50 mg of biomass (SF: 140–250 μm) with 100 mL of U(VI) solution at fixed initial concentration (10–100 mg/L) and pH 5.0. The flasks were agitated on a shaker at 150 rpm while keeping the temperature at 293, 303, or 313 K, respectively. Samples were collected and filtered after a 24 h of contact time. The amount of U(VI) adsorbed per unit of sorbent mass at equilibrium (q_e mg/g) was calculated by the mass balance equation:

$$q_e = \frac{V \times (C_0 - C_e)}{W}, \tag{1}$$

where C_0 and C_e are the concentrations of U(VI) ions in the initial solution and equilibrium solution (mg/L), respectively, V is the volume of the aqueous solution (L), and W is the mass of the resins (g).

Sorption kinetics

Sorption kinetics was obtained by contact of 500 mL of solution (at pH 5 and 293 K) with a given amount of biosorbents, under agitation at the velocity of 150 rpm/min. Since all these parameters (metal concentration, particle size, sorbent dosage, etc.) have been varied, the experimental conditions will be reported in the caption of the figures. Samples (about 1 mL) were collected at time intervals, filtered and analyzed for residual U(VI) concentration to obtain kinetic profiles.

Results and discussion

Sorbents characterization

The major components of PWS are cellulose, hemicellulose and lignin. Phosphorylation of the PWS converts the hydroxyl groups of PWS into phosphate groups through the esterification of the alcoholic groups by phosphoric acid according to the following reaction:

$$R - OH + H_3PO_4 \rightarrow R - OPO_3H^- + H_3O^+.$$
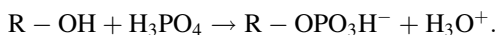
The semi-quantitative analysis from the energy dispersive X-ray spectroscopy revealed an atomic percentage of phosphorus in the phosphate-modified PWS (PA-PWS) of 1.9 % (or 1.27 mmol phosphate groups/g adsorbent). The zeta potential measurements for PA-PWS showed that the point of zero charge (pzc) of PA-PWS occurs at pH 6.2. As the pH increases, the zeta potential of PA-PWS decreases gradually and becomes negative at pH > 6.2, indicating the change of the surface charge of the bio-sorbents to basic character.

Figure 1 shows the FT-IR spectra for PWS (Fig. 1a), and PA-PWS before and after U(VI) biosorption (Fig. 1b, c). The broad band in the range of 3,700–3,000 cm^{-1} with the peak at 3,340 cm^{-1} is representative of the convolution of the signals for different vibration modes such as free OH, O–H stretch, and inter-chains H-bonds. The peak around 2,890 cm^{-1} is attributed to –CH stretching vibration [21]. It is generally difficult to find useful information from 4,000–2,000 cm^{-1} and thus spectrum analysis is generally focused on the 2,000–600 cm^{-1} regions. The band close to 1,645 cm^{-1} is probably due to the convolution of C=O stretch in conjugated p-substituted aryl ketones and those relevant to other compounds of the
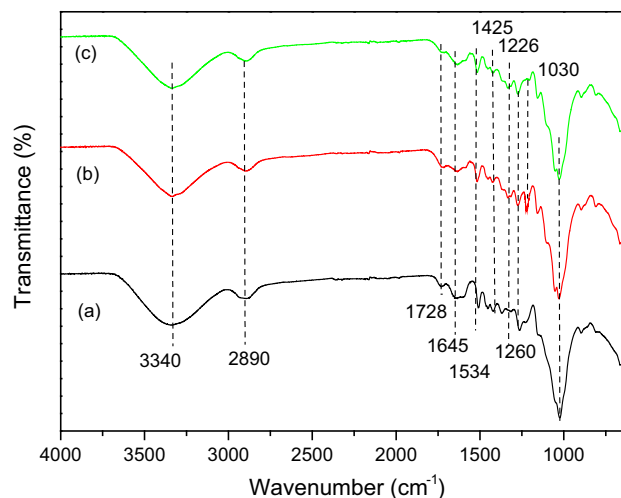

Fig. 1 FT-IR spectroscopy spectra for PWS (**a**), and PA-PWS before (**b**) and after (**c**) U(VI) biosorption

biomass (fucoidan or cellulose) [21]. The shoulder peak observed at 1,728 cm^{-1} is representative of either C=O stretch in unconjugated ketones, carbonyls, and in ester groups (especially in carbohydrates) conjugated aldehydes and carboxylic acids, or C=O valence vibration of acetyl and COOH groups. The peak at 1,534 cm^{-1} can be identified in amine/amide groups and in carboxyl groups. The peaks observed in the range 1,421–1,429 cm^{-1} correspond to the C–OH deformation vibration with contribution of the O–C–O symmetric stretching of carboxylate groups [22]. Significant decrease in the peak at 1,226 cm^{-1} corresponding to –P=O stretching vibration [19, 23] in the spectrum of PA-PWS after uranium adsorption indicates that phosphate groups are affected due to the adsorption process. Phosphate groups are known to have good ability for chelating uranium. FTIR spectroscopic characterization of the chitosan-tripolyphosphate (CTPP) beads showed that the phosphate groups may be the main active sites for the adsorption of uranium on CTPP beads [19]. However, no obvious change was observed in the major peaks (3,340 and 1,030 cm^{-1}) corresponding to hydroxyl groups. Other changes for PA-PWS after adsorption mainly consist in a shift of bands around 1,645 cm^{-1} (which moved from 1,646 to 1,637 cm^{-1}) and around 1,425 cm^{-1} (which moved from 1,430 to 1,423 cm^{-1}). These bands are the characteristic peaks of carboxylic acid groups, this is a confirmation that uranium binding also occurs on these specific reactive groups. Zou et al. [24] also stated that the carboxyl groups on the surface of the modified pine sawdust (CAMPS) were primarily responsible for the sorption of U(VI). In addition, several reactive groups have been identified from FTIR spectra for U(VI) sorption on citrus waste biomass: carboxyl, carbonyl and amide groups [16]. The results on this study as well as other works [16, 19, 24]

indicate that both the carboxyl groups and the phosphate groups may be responsible for the adsorption of U(VI) onto PA-PWS. The further detail characterization of the sorbents for elucidating the adsorption mechanism is currently conducted.

pH effect on U(VI) sorption

Figure 2 shows the pH impact on sorption capacity. Uranium sorption was affected by the change in pH and maximum uptake was observed at pH 5–5.5. Mechanisms such as ion exchange and complexation could play an important role in the sorption of U(VI) [17–19]. The multiple phosphate groups present in PA-PWS are the main active sites for U(VI) complexation [19]. The pH_{ZPC} of PA-PWS is close to 6.2. This means that in neutral and acid solutions this sorbent is positively charged. Under acidic conditions, the reactive groups are protonated due to the competition effect of protons and these reactive groups are not available for U(VI) binding. However, increasing the pH reduces the density of positive charges and the repulsion effect for the binding of U(VI) ions. At higher pH (pH > 5.5), the slight decrease of U(VI) sorption probably due to the hydrolysis of UO_2^{2+} to $[UO_2OH]^+$ [16], which results in lower affinity of the hydrolysed species for the phosphorylated PWS. This is expected since electrostatic interactions play a significant role in the formation of surface complexes between cations (UO_2^{2+} and $[UO_2OH]^+$) and the phosphorylated biomass sorbents [23].

The sorption capacity increases with pH within the range of pH 2–5 but decreases with sorbent dosage (Fig. 1). It should be noted that the stabilization of sorption capacity observed at sorbent dosage (SD) of 1.5 g/L on this figure is due to the complete recovery of the uranium from the solution and it is not indicative of the maximum sorption capacity of the material for given pH values. As highest sorption capacity for U(VI) sorption occurred at pH 5 and SD of 0.5 g/L, all subsequent experiments were carried out at these conditions.

Sorption isotherms

Sorption isotherms represent the solute distribution at equilibrium between the sorbent and the solution. The models of Langmuir and Freundlich are the most commonly used for describing the sorption isotherms. The Langmuir model is characterized by an asymptotic shape while the Freundlich model supposes an exponential trend. As shown in Fig. 3, the sorption capacity of U(VI) onto the PA-PWS tended to be an asymptotic value. The Langmuir and Freundlich isotherm equations [12, 19] could be represented as follows:
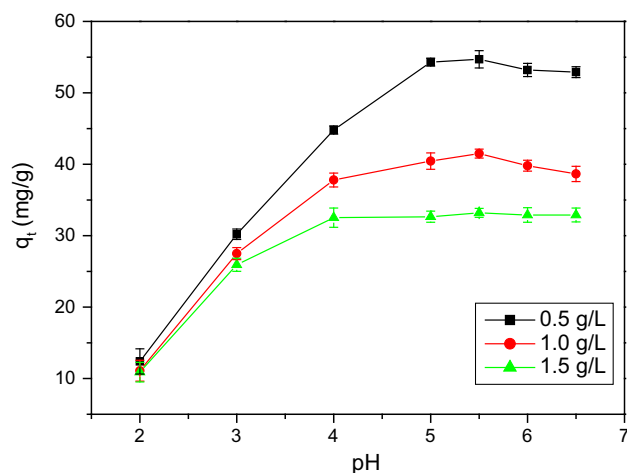

Fig. 2 Influence of pH on U(VI) sorption capacity using PA-PWS biosorbent (C_0: 50 mg/L; sorbent dosage: 0.5–1.5 g/L; particle size: 80–140 μm; temperature: 293 K; time: 24 h)

The Langmuir isotherm:
$$\frac{C_e}{q_e} = \frac{C_e}{q_m} + \frac{1}{q_m K_L}, \qquad (2)$$

where C_e is the equilibrium concentration (mg/L), q_e is the adsorbed amount of U(VI) (mg/g), q_m is the maximum monolayer adsorption capacity (mg/g), and K_L is a constant related to the affinity of the binding sites (L/mg).

The Freundlich isotherm: $\ln q_e = \ln k_F + 1/n \ln C_e$, (3)

where K_F (mg/g) and n are Freundlich constants indicating adsorption capacity and intensity, respectively.

The isotherm model parameters (q_m and k_F, k_L and n) were calculated from the slope and intercept values of the straight lines of plotting C_e/q_e versus C_e or $\ln q_e$ versus
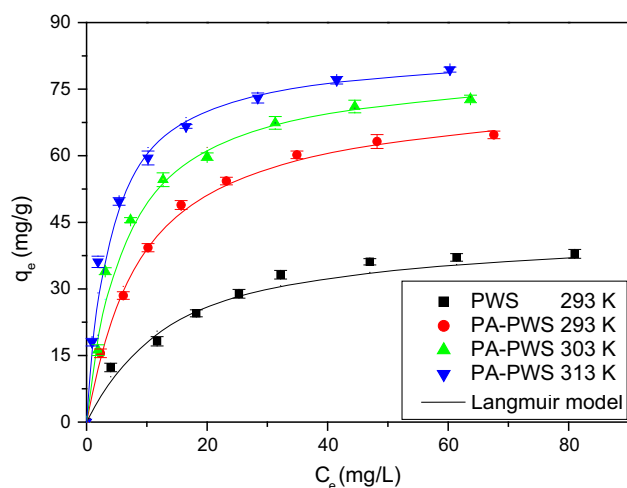

Fig. 3 U(VI) sorption isotherms using PA-PWS and PWS at different temperatures (C_0: 10–100 mg/L; sorbent dosage: 0.5 g/L; particle size: 80–140 μm; time: 24 h; pH 5)

Table 1 Adsorption isotherm parameters for the adsorption of U(VI) by PA-PWS and PWS (C_0: 10–100 mg/L; sorbent dosage: 0.5 g/L; particle size: 80–140 μm; time: 24 h; pH 5)

Sorbents	Temperature (K)	Langmuir parameters			Freundlich parameters		
		q_m (mg/g)	k_L (L/mg)	R^2	k_F (mg/g)	n	R^2
PA-PWS	313	84.7	0.277	0.9992	24.9	3.113	0.8960
	303	79.9	0.171	0.9981	18.2	2.671	0.8586
	293	74.1	0.115	0.9991	13.0	2.362	0.9312
PWS	293	44.8	0.075	0.9926	7.3	2.484	0.9588

ln C_e, respectively (see Suppl. Fig.1). The calculated values were given in Table 1. Based on the correlation coefficients, R^2, the adsorption of U(VI) ions correlated well with Langmuir isotherm equations. The sorption capacity increases with increasing temperature for PA-PWS, suggesting an endothermic process. Niu et al. [25] argued that the cation should be free from the shell of water molecules surrounding it for adsorbing onto the sorbent, thus the system required energy to remove these water molecules. If this energy is more than the energy released on binding of the cation onto the surface of the sorbent, then the entire sorption process is endothermic in nature.

The PA-PWS biosorbent is efficient for U(VI) recovery and has a maximum sorption capacity (q_m) of 74.1 mg/g (at 293 K), which is about 65 % higher than that of the untreated PWS (44.8 mg/g). According to the theory of hard and soft acids and bases (HSAB) defined by Pearson, the oxygen-donor adsorption sites of the sorbents can be classified as hard bases. These sites coordinate preferentially with actinide ions classified as hard acids. U(VI) ions can act as hard acids and form stronger complexes with oxygen-donor ligands present in the phosphate groups [19]. The chemical modification of the PWS improves its adsorption for U(VI) due to the introduction of phosphate groups. The q_m values of PA-PWS are compared to those of different sorbents reported in the literatures (Table 2). The PA-PWS shows a intermediary q_m (mg/g), which is higher than coffee residues [26], wheat straw [27], activated carbon [28], and biomass immobilized silica gel [29], but it is lower than wood powder [27], *Cyanobacterium bloom* [11], *Penicillium citrinum* [30], phosphorylated CF and CF coated with MnO [23]. It is noteworthy that the affinity coefficient (k_L = 0.115–0.277 L/mg) was relatively higher for PA-PWS compared to other biosorbents. In the case of U(VI) sorption using *Catenella repens*, Bhat et al. [13] obtained high sorption capacities (256 and 303 mg/g at pH 2.5 and 4.5, respectively) with the affinity coefficients of 0.01 and 0.12 L/mg for U(VI) at pH 2.5 and 4.5, respectively. For U(VI) sorption on citric acid modified pine sawdust, Zou et al. [24] found sorption capacities close to 71.6 mg/g with much lower affinity coefficient (close to 0.029 L/mg).

Table 2 Reported adsorption capacities of U(VI) by different adsorbents

Sorbents	U adsorption capacity (mg/g)	Refs.
Cyanobacterium bloom	246	[11]
Cactus fibres	62	[23]
Phosphorylated CF	107	
CF coated with MnO	110	
Coffee residues	40.5	[26]
Wheat straw	47.6	[27]
Wood powder	113	
Activated carbon	57.8	[28]
Biomass immobilized silica gel	50.3	[29]
Penicillium citrinum	274.7	[30]
PA-PWS	74.1	This work
PWS	44.8	

Table 3 Thermodynamic parameters for adsorption of U(VI) by PA-PWS at different temperatures

Sample	$\Delta H°$ (kJ/mol)	$\Delta S°$ (J/(mol K))	$\Delta G°$ (kJ/mol)		
			293 K	303 K	313 K
PA-PWS	33.46	199.01	−25.84	−27.83	−29.82

The thermodynamics such as enthalpy ($\Delta H°$, kJ/mol), entropy ($\Delta S°$, J/(mol K)), and Gibbs free energy ($\Delta G°$, kJ/mol) of U(VI) sorption were determined by correlation of the equilibrium constant according the Van't Hoff equation [33]:

$$\ln K_L = \frac{-\Delta H°}{RT} + \frac{\Delta S°}{R},$$ (4)

$$\Delta G° = \Delta H° - T\Delta S°,$$ (5)

where R is the gas constant, T is the solution temperature (K) and K_L is the Langmuir equilibrium constant (L/mol). $\Delta H°$ and $\Delta S°$ were obtained from the slope and intercept of the linear Van't Hoff plots of ln K_L versus 1/T: ln K_L = −4,025.2/
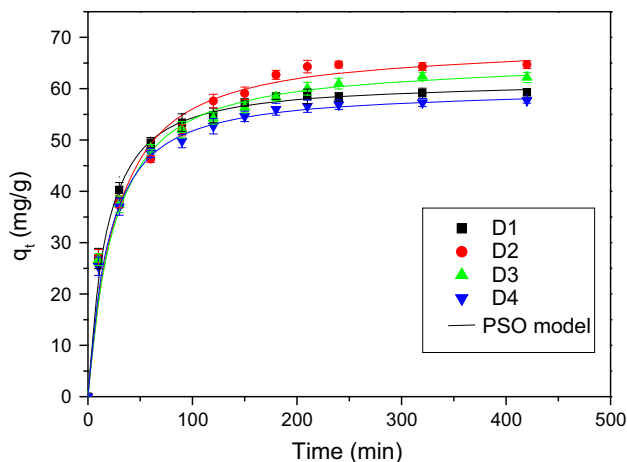
Fig. 4 Influence of particle size (*D*1: 0–80 μm; *D*2: 80–140 μm; *D*3: 140–250 μm; *D*4: 250–500 μm) on U(VI) uptake kinetics (*C*₀: 100 mg/L; sorbent dosage: 0.5 g/L; time: 7 h; pH 5 and 293 K)
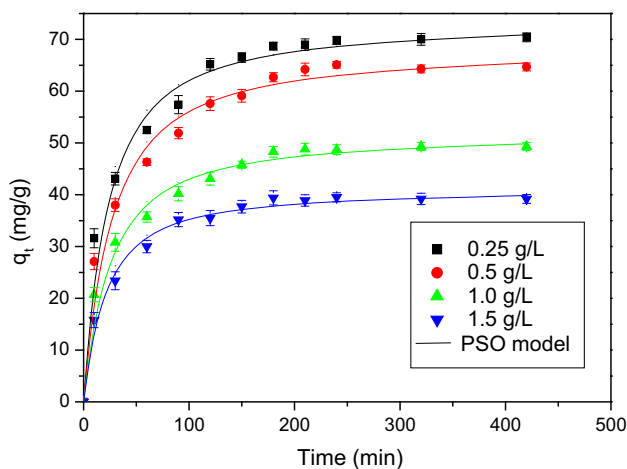

Fig. 5 Influence of sorbent dosage on U(VI) uptake kinetics (*C*₀: 100 mg/L; particle size: 80–140 μm; time: 7 h; pH 5 and 293 K)

$T + 23.937$ ($R^2 = 0.994$). The values of thermodynamic parameters were reported in Table 3. The positive value of ΔH^{o} confirms that the sorption is endothermic whereas the positive ΔS^{o} shows the increased randomness at the solid–solution interface during the adsorption process. The negative value of ΔG^{o} in Table 3 indicates that the adsorption reaction is spontaneous. Moreover, the decrease in the values of ΔG^{o} indicates that higher temperature favors the sorption process. Generally, the values of the thermodynamic parameters evaluated are close to corresponding values reported in literatures for similar systems [16, 23].

Sorption kinetics

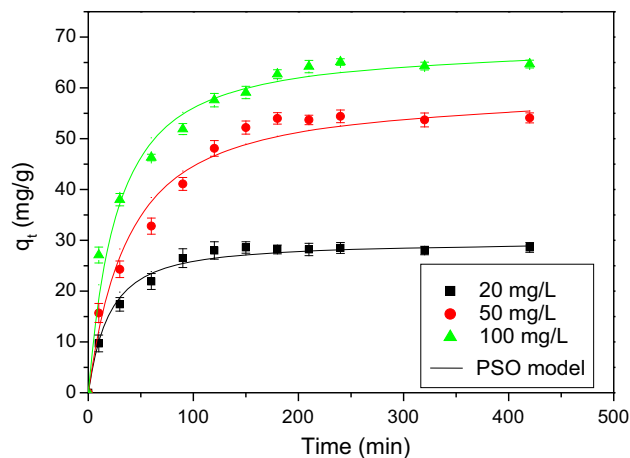The sorption kinetic process involves two stages: the initial rapid uptake stage followed by the slow uptake stage. As

Fig. 6 Influence of initial U(VI) concentration on U(VI) uptake kinetics (sorbent dosage: 0.5 g/L; particle size: 80–140 μm; time: 7 h; pH 5 and 293 K)

the concentration of the U(VI) from solution decreases the sorption process slows down and becomes constant. The sorption equilibrium could be achieved within 240 min (Figs. 4, 5, 6). The effects of particle size, sorbent dosage and metal concentration on uptake kinetics have been investigated and the kinetic profiles were fitted to various models including the pseudo-first order (PFO), Eq. (6), pseudo-second order (PSO), Eq. (7), and intra-particle diffusion, Eq. (8) [31, 32]:

$$\ln\left(q_e - q_t\right) = \ln q_e - k_1 t, \tag{6}$$

$$\frac{t}{q_t} = \frac{1}{k_2 q_e^2} + \frac{1}{q_e} t, \tag{7}$$

$$q_t = k_{\mathrm{int}} t^{1/2} + C, \tag{8}$$

where C is a constant, q_e and q_t (mg/g) refer to the amount of U(VI) ions adsorbed at equilibrium and at time (t), respectively; k_1 (min⁻¹), k_2 (g mg⁻¹ min⁻¹), and k_{int} (g mg⁻¹ min⁻¹/²) refer to the rate constant of the PFO, the PSO, and the intra-particle diffusion, respectively.

The values of q_e, k_1, k_2, and k_{int} were calculated from the slope and intercept values of the straight lines of plotting ln (q_e–q_t) versus time (t), t/q_t versus t, or q_t versus $t^{1/2}$, respectively (see Suppl. Figs. 2–4). The results of kinetic analysis are shown in Tables 4, 5, and 6. The PSO model allows approaching more accurately experimental data in all cases, as shown by the comparison of correlation coefficient. The PSO kinetic model assumes that the rate controlling step may be chemisorption, involving valence forces through sharing or exchange of electron between the U(VI) ions and adsorbents [19, 33]. The differences between experimental values and the modeled values of q_m obtained were <5 mg/g for the PSO model. The PFO model is not suitable for describing the adsorption kinetic since the theoretical q_e values calculated from this model

are much lower than the experimental data. Moreover, the PFO model could only be applicable over the initial stage of the adsorption process. The intra-particle diffusion model also could not fit well with the experimental results, this is an evidence that the resistance to intra-particle diffusion is probably not the limiting step for U(VI) sorption. In most cases, both the sorbent dosage and the metal concentration had great impact on the kinetic parameters (adsorption capacity and rate constant), while the particle size only had limited effect on these parameters (Tables 4, 5, 6). Since the PSO model showed the best fitting for describing the kinetic of U(VI) adsorption onto the PA-PWS, the following discussion was focused on this model.

Effect of particle size

The particle size of sorbents is an important parameter for determining the contribution of the resistance to intraparticle diffusion on the control of adsorption kinetics. As shown in Fig. 4, the kinetic profiles almost overlapped indicating that the particle size has a limited impact on mass transfer. The slightly lower adsorption capacity at equilibrium for $D1$ fraction (<80 μm) may be due to a partial degradation of the biomass during grinding operations. The experimental values of adsorption capacity ($q_{e, exp}$) decreased gradually with increasing particle size from $D2$ to $D4$. This is consistent with the theoretical values ($q_{e, cal}$) for PSO model (Table 4). Around 12.6 % decrease of $q_{e, cal}$ was observed between $D2$ and $D4$

fractions. The kinetic rate constant (k_2) also decreased with the particle size. However, the biggest difference of k_2 was observed between $D1$ and $D2$ (from 1.22×10^{-3} to 0.75×10^{-3} g mg^{-1} min^{-1}), while for the larger particles ($D2$–$D4$) the variation was rather limited (from 0.75×10^{-3} to $0.54 \times \times 10^{-3}$ g mg^{-1} min^{-1}).

The kinetic parameters of both k_1 and k_{int} increases with increasing particle size from $D1$ to $D2$, but decreases with particle size from $D2$ to $D4$. The variation of these kinetic parameters with the diameter of sorbent particles indicates that the external surface may play a part in the control of uptake kinetics.

Effect of sorbent dosage

The sorbent dosage affects the density of reactive groups available for metal adsorption and on the external surface area of the sorbent. Varying the sorbent dosage could thus change the adsorption kinetics. Figure 5 shows the kinetic profiles for PA-PWS under selected experimental conditions. The parameters of the kinetic models are summarized in Table 5. The equilibrium sorption capacity ($q_{e, cal}$) modeled by PSO model systematically overestimates the experimental values. The $q_{e, cal}$ values logically decreased with increasing sorbent dosage due to the lower rationale amount of adsorbates available for per unit of adsorbents when using higher sorbent dosage. On the other hand, the kinetic parameter, k_2, increased from 0.71×10^{-3} to 1.38×10^{-3} g mg^{-1} min^{-1} when the sorbent dosage

Table 4 Kinetic parameters of the adsorption of U(VI) onto PA-PWS at different particle size (C_0: 100 mg/L; sorbent dosage: 0.5 g/L; time: 7 h; pH 5 and 293 K)

PS (μm)	$q_{e\ exp}$ (mg/g)	Pseudo-first-order			Pseudo-second-order			Intraparticle diffusion	
		k_1 ($\times 10^{-2}$ min^{-1})	$q_{e\ cal}$ (mg/g)	R^2	k_2 ($\times 10^{-3}$ g/(mg min))	$q_{e\ cal}$ (mg/g)	R^2	k_{int} (mg/(g min$^{1/2}$))	R^2
0–80 ($D1$)	58.4	1.39	27.5	0.9416	1.22	61.7	0.9997	1.67	0.7312
80–140 ($D2$)	64.7	1.62	41.2	0.9339	0.75	68.9	0.9979	2.21	0.8401
140–250 ($D3$)	61.1	1.24	37.8	0.9901	0.72	65.7	0.9992	1.98	0.8373
250–500 ($D4$)	56.9	1.11	24.8	0.9395	0.54	60.2	0.9997	1.72	0.7683

Table 5 Kinetic parameters of the adsorption of U(VI) onto PA-PWS at different sorbent dosage (C_0: 100 mg/L; particle size: 80–140 μm; time: 7 h; pH 5 and 293 K)

Sorbent dosage (g/L)	$q_{e\ exp}$ (mg/g)	Pseudo-first-order			Pseudo-second-order			Intraparticle diffusion	
		k_1 ($\times 10^{-2}$ min^{-1})	$q_{e\ cal}$ (mg/g)	R^2	k_2 ($\times 10^{-3}$ g/mg/min)	$q_{e\ cal}$ (mg/g)	R^2	k_{int} (mg/(g min$^{1/2}$))	R^2
0.25	70.4	1.54	45.3	0.9889	0.71	74.1	0.9988	2.24	0.8151
0.5	64.7	1.62	41.2	0.9339	0.75	68.9	0.9979	2.22	0.8401
1.0	49.3	1.32	32.1	0.9745	0.90	52.3	0.9984	1.63	0.8337
1.5	39.2	1.31	18.8	0.8417	1.38	41.5	0.9985	1.31	0.7595

Table 6 Kinetic parameters of the adsorption of U(VI) onto PA-PWS at different U(VI) concentration (sorbent dosage: 0.5 g/L; particle size: 80–140 μm; time: 7 h; pH 5 and 293 K)

Conc. (mg/L)	$q_{e\ exp}$ (mg/g)	Pseudo-first-order			Pseudo-second-order			Intraparticle diffusion	
		k_1 ($\times 10^{-2}$ min^{-1})	$q_{e\ cal}$ (mg/g)	R^2	k_2 ($\times 10^{-3}$ g/mg/min)	$q_{e\ cal}$ (mg/g)	R^2	k_{int} (mg/(g min$^{1/2}$))	R^2
20	28.5	1.51	16.2	0.8469	2.17	29.9	0.9978	1.57	0.8196
50	54.3	1.45	37.4	0.8324	0.93	59.8	0.9930	3.25	0.9222
100	64.7	1.62	41.2	0.9339	0.75	68.9	0.9979	3.47	0.8861

increased from 0.25 to 1.5 g/L. The k_2 values are lower than those cited for uranium(VI) sorption using other biosorbents: 4.9×10^{-3}–5.5×10^{-3} g mg^{-1} min^{-1} for *Catenella repens* (a red alga) [13] and 0.26–0.36 g mg^{-1} min^{-1} for *Pseudomonas putida* [34], respectively.

In contrast with the trend of k_2 variation, the k_{int} values calculated from the intra-particle diffusion model decreased with increasing the sorbent dosage. However, no clear trend could be found for k_1 values. The variation of the kinetic rate constants shows that the sorbent dosage has an important impact on the control of uptake kinetics.

Effect of metal concentration

The initial U(VI) concentration was varied between 20 and 100 mg/L, the uptake kinetic curves are shown in Fig. 6. The equilibrium sorption capacity obviously increased with U(VI) concentration (Table 6). The q_e values increase with the concentration of U(VI) ions, whereas the values of k_2 decrease. Hence at lower U(VI) concentrations, the probability to get bonded on the active sites of the sorbents increases. Increasing the initial concentration may impact the concentration gradient between the solution and the internal reactive groups; which, in turn, may affect the kinetic rate for U(VI) adsorption. This may partly explain the variation of the kinetic rate with U(VI) concentration. In this case, the kinetic parameter, k_2, decreased with increasing metal concentration, consistently with another work on Cd(II) biosorption onto marine macroalgae biosorbent [35]. A similar trend was also found for U(VI) sorption onto CTS-g-PMAA/Bent [9]: the k_2 values decreased from 1.75×10^{-3} to 0.49×10^{-3} g mg^{-1} min^{-1} when the initial U(VI) concentration increased from 100 to 250 mg/L.

In the case of the intra-particle diffusion model, the k_{int} values calculated from this model increased with increasing the initial U(VI) concentration. However, the variation in the kinetic rate constants for the PFO model did not show a clear trend. The kinetic parameter, k_1, changes from 1.51×10^{-2} min^{-1}, 1.45×10^{-2} min^{-1} to 1.62×10^{-2} min^{-1} with increasing the U(VI) concentration from 20, 50 to 100 mg/L.

Conclusion

The phosphate-modified PWS (PA-PWS) is an efficient biosorbent for uranium(VI) sorption. Uranium uptake was affected by the change in pH and maximum uptake was observed at pH 5–5.5. The sorption isotherms are characterized by asymptotic shape and could be preferentially described by the Langmuir model rather than the Freundlich model. The maximum sorption capacity (q_m) increases with increasing temperature, indicating the endothermic nature of the sorption process. The q_m values reach 44.8 mg/g for the untreated PWS and 74.1 mg/g for PA-PWS at 293 K, respectively. Adsorption kinetics could be fitted well with the pseudo-second-order (PSO) rate equations. The particle size has a limited impact on the uptake profiles, indicating that the intraparticle diffusion is probably not the predominant controlling step in the sorption process. The equilibrium sorption capacity decreased with increasing sorbent dosage but increased with U(VI) concentration. The kinetic rate constant (k_2 for PSO) decreased with the average diameter of sorbent particles and the concentration, but increased with sorbent dosage. However, no clear trend was found for k_1 values. As shown by FT-IR analysis, the U(VI) sorption occurs mainly through interactions with phosphate groups and carboxylic acid groups of PA-PWS.

References

1. Sztajnkrycer MD, Otten EJ (2004) Chemical and radiological toxicity of depleted uranium. Mil Med 169:212–216
2. Saini AS, Melo JS (2013) Biosorption of uranium by melanin: kinetic, equilibrium and thermodynamic studies. Bioresour Technol 149:155–162
3. Liu M, Dong F, Yan X, Zeng W, Hou L, Pang X (2010) Biosorption of uranium by *Saccharomyces cerevisiae* and surface

interactions under culture conditions. Bioresour Technol 101:8573–8580

4. Mellah A, Chegrouche S, Barkat M (2007) The precipitation of ammonium uranyl carbonate (AUC): thermodynamic and kinetic investigations. Hydrometallurgy 85:163–171

5. Gu B, Ku Y, Brown G (2005) Sorption and desorption of perchlorate and U(VI) by strong-base anion-exchange resins. Environ Sci Technol 39:901–907

6. Jyothi A, Rao GN (1990) Solvent extraction behaviour of lanthanum(III), cerium(III), europium(III), thorium(IV) and uranium(VI) with 3-phenyl-4-benzoyl-5-isoxazolone. Talanta 37:431–433

7. Hur Y, Lee Y, Jang G, Choi H, Koh K (2002) Detection of uranyl ion using polymeric membrane containing calyx[6] arene uranophile. Mol Cryst Liq Cryst 377:221–224

8. Rui X, Kwon M, Loughlin E, Dunham-Cheatham S, Fein J, Bunker B (2013) Bioreduction of hydrogen uranyl phosphate: mechanisms and U(IV) products. Environ Sci Technol 47:5668–5678

9. Anirudhan TS, Rijith S (2012) Synthesis and characterization of carboxyl terminated poly(methacrylic acid) grafted chitosan/bentonite composite and its application for the recovery of uranium(VI) from aqueous media. J Environ Radioact 106:8–19

10. Srivastava S, Bhainsa KC, Dsouza SF (2010) Investigation of uranium accumulation potential and biochemical responses of an aquatic weed *Hydrilla verticillata* (L.f.) Royle. Bioresour Technol 101:2573–2579

11. Li P, Mao Z, Rao X, Wang X, Min M, Qiu L, Liu Z (2004) Biosorption of uranium by lake-harvested biomass from a *Cyanobacterium bloom*. Bioresour Technol 94:193–195

12. Sar P, Dsouza SF (2001) Biosorptive uranium uptake by a *Pseudomonas strain*: characterization and equilibrium studies. J Chem Technol Biotechnol 76:1286–1294

13. Bhat SV, Melo JS, Chaugule BB, Dsouza SF (2008) Biosorption characteristics of uranium(VI) from aqueous medium onto *Catenella repens*, a red alga. J Hazard Mater 158:628–635

14. Dubois MA, Dozol JF, Nicotra C, Serose J, Massiani C (1995) Pyrolysis and incineration of cationic and anionic ion-exchange resins—identification of volatile degradation compounds. J Anal Appl Pyrol 31:129–140

15. Konstantinou M, Pashalidis I (2007) Adsorption of hexavalent uranium on biomass by-product. J Radioanal Nucl Chem 273:2095–2102

16. Saleem N, Bhatti HN (2011) Adsorptive removal and recovery of U(VI) by citrus waste biomass. Bioresources 6:2522–2538

17. Sciban M, Radetic B, Kevresan Z, Klasnja M (2007) Adsorption of heavy metals from electroplating wastewater by wood sawdust. Bioresour Technol 98:402–409

18. Zhang H, Tang Y, Liu XN, Ke ZG, Su X, Cai DQ, Wang XQ, Liu YD, Huang Q, Yu ZL (2011) Improved adsorptive capacity of pine wood decayed by fungi *Poria cocos* for removal of malachite green from aqueous solutions. Desalination 274:97

19. Sureshkumar MK, Das D, Mallia MB, Gupt PC (2010) Adsorption of uranium from aqueous solution using chitosan-tripolyphosphate (CTPP) beads. J Hazard Mater 184:65–72

20. Musina Y, Goring D (1974) Klanson and acid-soluble lignin content of hardwoods. Wood Sci 7:133–134

21. Schwanninger M, Rodrigues JC, Pereira H, Hinterstoisser B (2004) Effects of short time vibratory ball milling on the shape of FT-IR spectra of wood and cellulose. Vib Spectrosc 36:23–40

22. Åkerholm M, Salmén L (2001) Interactions between wood polymers studied by dynamic FT-IR spectroscopy. Polymer 42:963–969

23. Prodromou M, Pashalidis I (2013) Uranium adsorption by nontreated and chemically modified cactus fibres in aqueous solutions. J Radioanal Nucl Chem 298:1587–1595

24. Zou WH, Zhao L (2012) Removal of uranium(VI) from aqueous solution using citric acid modified pine sawdust: batch and column studies. J Radioanal Nucl Chem 292:585–595

25. Niu Z, Fan Q, Wang W, Xu J, Chen L, Wu W (2009) Effect of pH, ionic strength and humic acid on the sorption of uranium(VI) to attapulgite. Appl Radiat Isot 67:1582–1590

26. Mahramanlioglu M, Bicer IO, Misirli T, Kilislioglu A (2007) Removal of uranium by the adsorbents produced from coffee residues. J Radioanal Nucl Chem 273:621–624

27. Bagherifam S, Lakzian A, Ahmedi SJ, Rahimi MF, Halajnia A (2010) Uranium removal from aqueous solutions by wood powder and wheat straw. J Radioanal Nucl Chem 392:283–289

28. Kütahyali C, Eral M (2010) Sorption studies of uranium and thorium on activated carbon prepared from olive stones: kinetic and thermodynamic aspects. J Nucl Mater 396:251–256

29. Aytas S, Turkozu DA, Gok C (2011) Biosorption of uranium(VI) by bifunctionalized low cost biocomposite adsorbent. Desalination 280:354–362

30. Pang C, Liu YH, Cao XH, Li M, Huang GL, Hua R, Wang CX, Liu YT, An XF (2011) Biosorption of uranium(VI) from aqueous solution by dead fungal biomass of Penicillium citrinum. Chem Eng J 170:1–6

31. Akkaya R (2013) Removal of radioactive elements from aqueous solutions by adsorption onto polyacrylamide–expanded perlite: equilibrium, kinetic, and thermodynamic study. Desalination 321:3–8

32. Ho YS, Mckay G (1999) Pseudo-second-order model for sorption process. Process Biochem 34:451–465

33. Zhou LM, Shang C, Liu ZR, Huang GL, Adesina AA (2012) Selective adsorption of uranium(VI) from aqueous solutions using the ion-imprintedmagnetic chitosan resins. J Colloid Interface Sci 366:165–172

34. Choi J, Ju Lee Y, Yang JS (2009) Biosorption of heavy metals and uranium by starfish and *Pseudomonas putida*. J Hazard Mater 161:157–162

35. Herrero R, Lodeiro P, Rojo R, Ciorba A, Rodriguez P (2008) Biosorption of cadmium by biomass of brown marine macro algae. Bioresour Technol 99:4138–4146